previously reported observation that only five HRP-positive cells were visualized after the marker enzyme was injected into a pain-sensitive structure, tooth pulp (*17*), supports this notion. Nevertheless, limited numbers of HRP-positive cells found in our studies may reflect differences between species (cat versus human), the relatively small area to which HRP was applied, the wide receptive fields from which trigeminal neurons project (*16*), or perhaps the uptake properties of these nerve terminals. The possibility that other cranial nerves convey sensory information from meningeal blood vessels also deserves consideration. By "painting" HRP mixed with a polymer directly onto the surface of the middle cerebral artery, uptake of the marker by perivascular nerve endings was assured. In this instance, uptake presumably occurred within myelinated and poorly myelinated neurons surrounding large cerebral arteries (*18*).

MARC MAYBERG
Department of Nutrition and Food Science, Massachusetts Institute of Technology, Cambridge 02139, and *Department of Neurosurgery, Massachusetts General Hospital, Boston 02114*

ROBERT S. LANGER
Department of Nutrition and Food Science, Massachusetts Institute of Technology, and *Department of Surgery, Children's Hospital Medical Center, Boston, Massachusetts 02115*

NICHOLAS T. ZERVAS
Department of Neurosurgery, Massachusetts General Hospital

MICHAEL A. MOSKOWITZ*
Department of Nutrition and Food Science, Massachusetts Institute of Technology, and *Section of Neurology, Department of Medicine, Brigham and Women's Hospital, Harvard Medical School, Boston, Massachusetts 02115*

References and Notes

1. B. S. Ray and H. G. Wolff, *Arch. Surg. (Chicago)* **41**, 813 (1940); F. L. McNaughton, *Res. Publ. Assoc. Res. Nerv. Ment. Dis.* **18**, 178 (1938); H. G. Wolff, *Headache and Other Head Pain* (Oxford Univ. Press, New York, 1963).
2. M. A. Moskowitz, J. F. Reinhard, J. Romero, E. Melamed, D. Pettibone, *Lancet* **1979-II**, 883 (1979).
3. J. H. LaVail and M. M. LaVail, *Science* **176**, 1416 (1972).
4. The cats were anesthetized with subcutaneous ketamine hydrochloride (20 mg/kg) and intraperitoneal sodium pentobarbital (5 mg/kg). Under the operating microscope, a right subtemporal and subfrontal approach enabled the middle cerebral artery to be exposed at its origin from the internal carotid artery. The floor of the middle cranial fossa was covered with a sheet of polyethylene to prevent any contact between the coated vessel and the underlying trigeminal ganglia. After HRP was applied to the vessel embedded in the polymer, this mixture was sealed from adjacent structures with polyethylene film and petrolatum. The wound was closed and the animals were allowed to recover.
5. M. A. Moskowitz, M. Mayberg, R. S. Langer, *Brain Res.* **212**, 460 (1981).
6. C. W. Bowers and R. E. Zigmond, *J. Comp. Neurol.* **185**, 381 (1979).
7. M. M. Mesulam, *J. Histochem. Cytochem.* **26**, 106 (1978).
8. In one cat, HRP-containing polymer was applied to a 1-cm^2 area of parietal cortex (between the inferior and superior divisions of the middle cerebral artery) in an area devoid of large cerebral arteries. The animal was allowed to recover and was perfused with glutaraldehyde after 72 hours.
9. The right supraorbital nerve was exposed at its emergence from the supraorbital foramen and dissected free for 1 cm. The nerve was transected at this point and the proximal end was placed in the polyethylene tube containing a 50 percent solution of horseradish peroxidase (Sigma type VI) for 2 hours. After 48 hours, the ganglia were removed after perfusion and sectioned serially.
10. S. Gobel, *J. Neurocytol.* **3**, 219 (1974).
11. C. M. Fisher, in *Pathogenesis and Treatment of Cerebrovascular Disease*, W. Fields, Ed. (Thomas, Springfield, Va., 1960), pp. 123–164.
12. G. W. Pickering and W. Hess, *Clin. Sci.* **1**, 77 (1933); G. A. Schumacher, B. S. Ray, H. G. Wolff, *Arch. Neurol. Psychiatry* **44**, 701 (1940).
13. J. C. White and W. H. Sweet, *Pain: Its Mechanisms and Neurological Control* (Thomas, Springfield, Va., 1955).
14. B. Arvidson, *Acta Neuropathol.* **38**, 49 (1977); C. W. Morgan, E. Nadelhaft, W. C. de Groat, *Neurosurgery* **2**, 252 (1978).
15. H. Cushing, *Bull. Johns Hopkins Hosp.* **15**, 213 (1904).
16. K. V. Anderson and G. S. Pearl, *Exp. Neurol.* **47**, 357 (1975); G. S. Pearl, K. V. Anderson, H. S. Rosing, *ibid.* **54**, 432 (1977).
17. L. Furstman, S. Saporta, L. Kruger, *Brain Res.* **84**, 320 (1975).
18. G. C. Huber, *J. Comp. Neurol.* **9**, 1 (1899); S. Clarke, *ibid.* **60**, 21 (1929).
19. Supported by NIH grants NS 15201, HL 22573, and GM 26698. M.A.M. is an established investigator of the American Heart Association.
* Send requests for reprints to M.A.M. Present address: Departments of Neurology and Neurosurgery, Massachusetts General Hospital, Boston 02114.

1 August 1980; revised 18 December 1980

Freeze-Fracture Cytochemistry: Replicas of Critical Point–Dried Cells and Tissues After Fracture-Label

Abstract. *Applications of the new fracture-labeling techniques for the observation of cytochemical labels on platinum-carbon replicas are described. Frozen cells, embedded in a cross-linked protein matrix, and frozen tissues are fractured with a scalpel under liquid nitrogen, thawed, labeled, dehydrated by the critical point drying method, and replicated. This method allows direct, high-resolution, two-dimensional chemical and immunological characterization of the cellular membranes in situ, as well as detection of sites within cross-fractured cytoplasm and extracellular matrix.*

Face views of biological membranes are revealed in platinum-carbon replicas of freeze-fractured cells and tissues. The fracture process appears to split regions of the membrane having a bilayer organization (*1*). The bilayer continuum of biological membranes is interrupted by integral membrane proteins that may span the membrane. In freeze-fracture replicas, these proteins, and possibly their tightly associated lipids, interrupt the smooth fracture plane of the bilayer and appear as membrane particles. Characterization of the chemistry and topology of components represented by the membrane particles is derived from studies of freeze-etched surface-labeled membranes (*2*) and of recombinants of membrane lipids and integral proteins (*3*). The generalization of the correspondence between integral membrane proteins and membrane particles is therefore inferential and largely based on the qualitative homogeneity of the freeze-fracture morphology of all biological membranes.

The low temperature (below −100°C) and high vacuum (below 2×10^{-6} mmHg) at which the fracture faces are produced and replicated have limited the development of techniques for cytochemical characterization of the identity and distribution of fracture face components. We have developed methods that permit the cytochemical labeling of freeze-fractured cells and tissues and observation of the labels by thin-section electron microscopy (*4*). These thin-section fracture-labeling methods involve grinding (that is, multiple fracture) of frozen cells and tissues that are immersed in liquid nitrogen. The fractured specimens are thawed, labeled, and processed for thin sectioning. Initial application of this method to the labeling of freeze-fractured erythrocytes (*4*) showed that anionic and lectin binding sites can be labeled on the fracture faces. In particular, concanavalin A binding sites, associated in human erythrocytes to the band 3 component—a membrane-traversing protein and the principal component of the membrane particles—are partitioned during fracture in a manner similar to that of the particles: about 75 percent of the label is seen on the inner, protoplasmic face (*5*), and the rest is associated with the exoplasmic face of the membrane. This signifies that surface residues and chemical groups associated with integral membrane-traversing proteins may be dragged during fracture from their sites at the outer surface across the frozen outer half of the membrane. In addition, the process of fracture appears to cause exposure of additional chemical groups which in the in-

0036-8075/81/0710-0230$00.50/0

tact membrane might be sterically inaccessible or chemically unreactive, or both (*4*). We have applied these thin-section fracture-labeling methods to intact cells and tissues to label the fracture faces of plasma and intracellular membranes (*6*).

Thin-section fracture-labeling permits the distribution of the label to be related to the cellular and intracellular structures beneath the plane of fracture. To provide information of the two-dimensional distribution of the label and to relate the distribution of components to the conventional morphology of platinum-carbon replicas of freeze-fractured specimens, we have developed replica techniques to examine critical point–dried specimens after they are fracture-labeled.

For our experiments, we used human

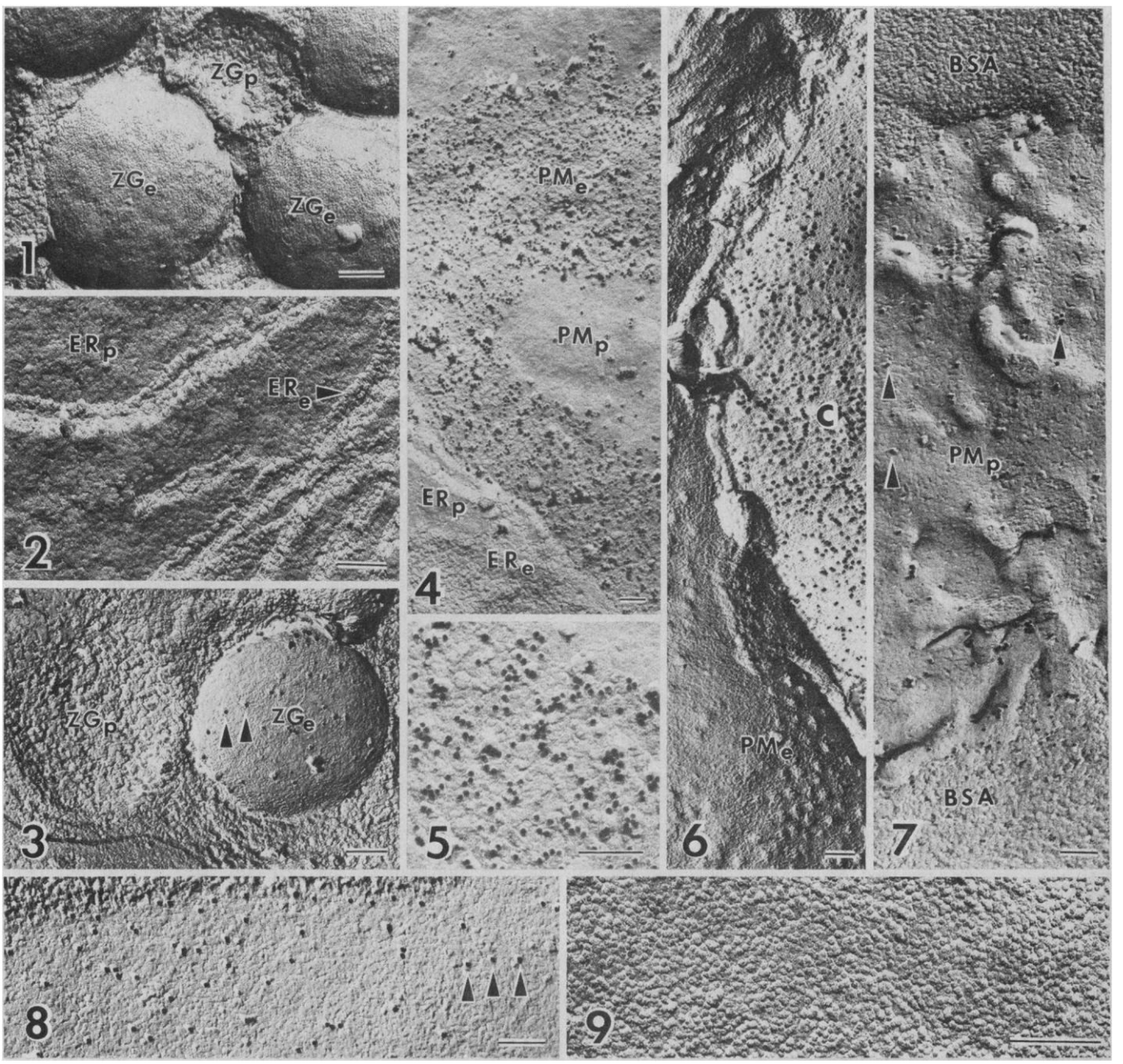

Figs. 1 and 2. Critical point–dried rat pancreas after freeze-fracturing. Protoplasmic and exoplasmic fracture faces of zymogen granule (ZG_p and ZG_e) and of endoplasmic reticulum membranes (ER_p and ER_e). Scale bars, 0.2 μm. Figs. 3 to 5. Localization of WGA binding sites on the fractured faces of pancreatic acinar cells. Fractured tissue was treated with WGA and labeled with colloidal gold–ovomucoid complex (*11*). In Fig. 3, colloidal gold particles (arrowheads) are sparsely distributed over the exoplasmic face of zymogen granules (ZG_e). In Fig. 4, colloidal gold particles are concentrated over the exoplasmic face of the lateral plasma membrane (PM_e), sparse over the protoplasmic face (PM_P), and virtually absent over fractured endoplasmic reticulum membranes (ER_p and ER_e). In Fig. 5, high magnification of a region from Fig. 4 shows the electron-opaque spherical colloidal gold granules and their shadows. The regular small step expected between the fracture faces of the lateral membranes of two adjacent cells is not evident; these faces are distinguished from each other by their different texture [see text and (*4*) for explanation]. Scale bars, 0.2 μm. Fig. 6. Localization of rat serum antigens on the fracture faces of a capillary within rat adenohypophysis parenchyma. Fractured tissue treated with antibody (IgG) to rat serum and labeled with colloidal gold–protein A complex (*11*). Colloidal gold granules are abundant over the plasma-containing, cross-fractured capillary lumen (*c*) and absent from the endothelial cell membrane faces (PM_e). Scale bar, 0.2 μm. Figs. 7 and 8. Colloidal gold particles (arrowheads) locate WGA bound to the protoplasmic faces of the plasma membrane of a freeze-fractured leukocyte (PM_p) (Fig. 7) and of a human erythrocyte (Fig. 8). Cells embedded in cross-linked bovine serum albumin gel (*BSA*). Scale bars, 0.2 μm. Fig. 9. Cationized ferritin molecules cover protoplasmic face of freeze-fractured human erythrocyte. Scale bar, 0.2 μm.

erythrocytes and leukocytes embedded in a cross-linked matrix of 30 percent bovine serum albumin (*4, 6*), as well as rat pancreas and adenohypophysis gland tissues. Erythrocytes and leukocytes were fixed in 0.5 to 1 percent glutaraldehyde for 30 minutes, and the tissues were fixed in 1 to 3 percent glutaraldehyde for 2 hours. Slices of gels and tissues were impregnated with 30 percent glycerol, frozen in Freon 22 (cooled by liquid nitrogen), and then immersed in liquid nitrogen and fractured with a scalpel. The fractured pieces were thawed in 30 percent glycerol with 0.5 percent glutaraldehyde, deglycerinated, and labeled. The tissue and gel fragments were then fixed in 1 percent OsO_4 for 30 minutes, dehydrated in ethanol, and subjected to critical point drying. Dried specimens were oriented on a specimen carrier and shadowed with a platinum-carbon gun. The replicas were floated and cleaned overnight in 5 percent sodium hypochlorite solution, rinsed in water, and collected on Formvar-coated grids.

The platinum-carbon replicas of these cells and tissues show that their original freeze-fractured appearance is retained to a remarkable degree. Cellular components as well as major ultrastructural elements are evident (Figs. 1 to 7). The degree of preservation of membrane faces depends on the quality of the physical support underneath: protoplasmic faces (Figs. 2 to 7) with the exception of those of zymogen granules (Figs. 1 and 3) are generally well preserved; exoplasmic faces (Figs. 2, 4, 5, and 6) are, in general, less well preserved because the components of the exoplasmic space on which they rest are less compact and offer less opportunities for cross-linkage during fixation (*4*). Exceptions are, for instance, the exoplasmic faces of pancreatic secretory granules, which are well preserved because they are backed by compacted secretory materials (Figs. 1 and 3). Finer ultrastructural detail is observed: capillary fenestrae are clear (Fig. 6) and so are nuclear pores and tight junctions (*7*).

The fine structure of the protoplasmic faces of critical point–dried, fractured membranes (Figs. 7 and 8) is different from that of conventional freeze-fractured replicas. Membrane particles observed against a smooth background are replaced by rugous faces whose background texture as well as ultrastructural features are characteristic of each membrane—compare the protoplasmic faces of erythrocytes (Fig. 8) and leukocytes (Fig. 7). This different ultrastructure appears to result from reorganization of membrane components (mainly membrane lipids) upon thawing in an aqueous environment (*4, 8*). In consequence, the fracture faces observed in platinum-carbon replicas of preparations that are freeze-fractured, thawed, and subjected to critical point drying are not strictly equivalent to conventional freeze-fractured faces. Thus, although the conventional nomenclature of freeze-fractured faces (*5*) is used here, interpretation of the results must take into account the possibility of reorganization of membrane components after membrane splitting.

In human erythrocytes, cationized ferritin (*9*) binds to both protoplasmic and exoplasmic faces, as seen in thin sections of fracture-labeled preparations (*4*). We show now that cationized ferritin molecules can also be identified as a dense cover of globular 13-nm entities on the protoplasmic faces of the critical point–dried, freeze-fractured erythrocytes (Fig. 9). Cationized ferritin binds, at least in part, to anionic sites revealed by the fracture process (*4*). Because cationized ferritin at *p*H 4.0 or colloidal iron cannot identify the chemical nature of the anionic groups, we used wheat germ agglutinin (WGA) to label possible sialic acid residues on the fracture faces (*10*). In addition, since platinum casts of ferritin molecules can be difficult to resolve against the rugous texture of the critical point–dried fracture faces, we used electron-opaque colloidal gold conjugates (*11*) as a less ambiguous marker. Colloidal gold particles resisted sodium hypochlorite digestion of the tissue during cleaning of the replica and remained trapped in the platinum-carbon cast. In replicas, each colloidal gold granule is observed as a 20-nm circular black granule accompanied by the shadow it casts onto the fracture face (Figs. 3, 5, 7, and 8).

Colloidal gold labeling of WGA binding sites (*10*) was achieved by incubation of the freeze-fractured, thawed specimens with the lectin (0.25 mg/ml for 30 minutes at 37°C), followed by washing and incubation in the presence of WGA-binding, ovomucoid-coated colloidal gold (3 hours at room temperature; overnight at 4°C). Preliminary experiments showed that, in the absence of WGA, ovomucoid-coated colloidal gold failed to bind to the fractured specimens. Controls consisted of fractured specimens incubated with WGA in the presence of 0.4*M* *N*-acetyl-D-glucosamine, rinsed, and labeled with ovomucoid-coated colloidal gold.

In erythrocyte membranes, most of the colloidal gold label is associated with the exoplasmic half of the fractured membrane, with about 10 to 20 percent of the label dispersed over the protoplasmic face (Fig. 8). In leukocytes also, most of the label is observed on the exoplasmic face, and the amount of label on the protoplasmic face is variable. In tissues, the differences in the labeling of protoplasmic and exoplasmic faces are clearest on fractured lateral plasma membranes, since the two faces can be seen adjacent to each other in a single fractured area (Figs. 4 and 5). Within the cell, colloidal gold–ovomucoid conjugates do not label the membranes of fractured endoplasmic reticulum (Fig. 4) and nuclear envelopes (*7*). The exoplasmic faces of pancreatic secretory granules are sparsely labeled [arrowheads in Fig. 3 (ZG_e)] in contrast to the virtual absence of label on the protoplasmic faces.

Labeling of the protoplasmic face of erythrocyte membranes by WGA–ovomucoid-coated colloidal gold shows that a proportion of the oligosaccharides originally exposed at the outer surface and associated with the transmembrane protein glycophorin (*12*) can be dragged, during freeze-fracture, across the outer half of the membrane to partition with the inner, protoplasmic, half. In human leukocytes, variable WGA labeling of the protoplasmic face indicates the presence of variable proportions of integral membrane components with similar behavior. The presence of surface marker on exoplasmic faces of fracture-labeled membranes is difficult to interpret. It may be a result of reorganization of membrane components upon thawing (discussed above) or a result of attachment of the label, through defects on the thawed fracture face, to components at the outer membrane surface. These problems are aggravated because the exoplasmic half of fractured membranes is poorly stabilized against the gels or interstitial spaces.

Fracture-labeling can also be used to locate tissue antigens. For these experiments we coated colloidal gold with protein A (*13*), a molecule that binds to the Fc fragment of immunoglobulin G (IgG). We treated freeze-fractured rat adenohypophysis, a tissue particularly rich in capillaries, with goat antibodies (IgG fraction) to rat serum and then with colloidal gold–protein A. As expected, the label was confined to the lumen of cross-fractured capillary vessels (Fig. 6); none was observed on the fractured membranes of the endothelial cell and very few within the cytoplasm.

Our results show that cytochemical methods can be used to label the faces produced by freeze-fracturing of cells and tissues. They confirm our view that important surface groups of biological membranes (those with WGA and concanavalin A binding sites) may partition, during fracture, with the protoplasmic half of the membrane (*4*). We believe that these groups are part of integral membrane-transversing proteins that are dragged from the outer surface across the exoplasmic half of the membrane. In addition, splitting of the bilayer membrane continuum renders accessible for cytochemical labeling other groups associated at the outer surface with components that, upon fracture, partition with the exoplasmic half: lipid molecules of the outer half of the bilayer, peripheral membrane proteins at the outer surface, and putative integral proteins associated with the exoplasmic half. In consequence, fracture-labeling in its two forms (thin section and critical point drying) appears to provide a method for the identification of surface sites (including antigens and receptors) associated with transmembrane molecules or oligomeric complexes, as well as for the structural and cytochemical dissection of plasma and intracellular membranes.

PEDRO PINTO DA SILVA*
BECHARA KACHAR
MARIA ROSARIA TORRISI
CHARLES BROWN
CLIFFORD PARKISON

Laboratory of Pathophysiology, National Cancer Institute, National Institutes of Health, Bethesda, Maryland 20205

References and Notes

1. D. Branton, *Proc. Natl. Acad. Sci. U.S.A.* **55**, 1048 (1966); P. Pinto da Silva and D. Branton, *J. Cell Biol.* **45**, 598 (1970).
2. P. Pinto da Silva, S. D. Douglas, D. Branton, *Nature (London)* **232**, 104 (1971); V. T. Marchesi *et al.*, *Proc. Natl. Acad. Sci. U.S.A.* **69**, 1445 (1972); T. W. Tillack, R. E. Scott, V. T. Marchesi, *J. Exp. Med.* **135**, 1209 (1972); P. Pinto da Silva, P. Moss, H. H. Fudenberg, *Exp. Cell Res.* **81**, 127 (1973); P. Pinto da Silva and G. L. Nicolson, *Biochim. Biophys. Acta* **363**, 311 (1974).
3. P. Pinto da Silva and D. Branton. *Chem. Phys. Lipids* **8**, 265 (1972); K. Hong and W. Hubbell, *Proc. Natl. Acad. Sci. U.S.A.* **69**, 2617 (1972); C. W. M. Grant and H. M. McConnell, *ibid.* **71**, 4653 (1974); J. P. Segrest, T. Gulik-Krzywicki, C. Sardet, *ibid.*, p. 3294; W. Kleemann and H. M. McConnell, *Biochim. Biophys. Acta* **419**, 206 (1976).
4. P. Pinto da Silva, C. Parkison, N. Dwyer, *Proc. Natl. Acad. Sci. U.S.A.* **78**, 343 (1981).
5. D. Branton *et al.*, *Science* **190**, 54 (1975).
6. P. Pinto da Silva, C. Parkison, N. Dwyer, *J. Histochem. Cytochem.*, in press.
7. P. Pinto da Silva, M. R. Torrisi, B. Kachar, in preparation; P. Pinto da Silva and M. R. Torrisi, in preparation.
8. The observation of an interrupted unit membrane (trilaminar) profile in thin sections of freeze-fractured, thawed membranes supports this interpretation. The unilamellar profile expected from a split bilayer membrane was observed only in gels freeze-substituted in osmium-acetone [see figure 1f in (*4*)], that is, under conditions of maximum lipid stabilization. Unfortunately, cytochemical labels cannot be used in osmium-fixed, freeze-substituted preparations.
9. D. Danon, L. Goldstein, E. Marikovsky, E. Skutelsky, *J. Ultrastruct. Res.* **38**, 500 (1972).
10. B. P. Peters, S. Ebisu, I. J. Goldstein, M. Flashner, *Biochemistry* **18**, 5505 (1979).
11. G. A. Ackerman, *Anat. Rec.* **195**, 641 (1979).
12. V. T. Marchesi, *Semin. Hematol.* **16**, 3 (1979); T. L. Steck, *J. Supramol. Struct.* **8**, 311 (1978).
13. E. L. Romano and M. Romano, *Immunochemistry* **14**, 711 (1977); J. Roth, M. Bendayan, L. Orci, *J. Histochem. Cytochem.* **26**, 1074 (1978).

* Address reprint requests to Laboratory of Pathology, Building 10, Room 5B50, National Cancer Institute, Bethesda, Md. 20205.

23 December 1980; revised 3 March 1981

Serum Albumin Beads: An Injectable, Biodegradable System for the Sustained Release of Drugs

Abstract. *Biologically active compounds were entrapped in cross-linked serum albumin microbeads. Injection of these drug-impregnated beads into rabbits produced no adverse immunological reactions. Sustained release (20 days) of progesterone was demonstrated in vivo.*

The formulation of a device for controlled release of biologically active substances has been the goal of many researchers (*1*). For injectable preparations, it is advantageous to use for the matrix a material that can be assimilated. The matrix should not produce adverse immunological reactions, and the matrix material should be readily available and relatively inexpensive. Albumin is such a material; its concentration in the serum of higher mammals is high, 40 to 50 mg/ml, and it can be prepared from outdated blood by well-known fractionation methods (*2*). Injectable beads prepared from albumin under mild conditions should yield a nonimmunogenic, biodegradable device for drug delivery. Since native serum albumin binds many drugs strongly (*3*), this binding would in itself retard drug release from an injection site until the albumin is degraded by proteolytic enzymes. We used albumin beads prepared by chemical cross-linking of the protein as a device for the controlled release of progesterone in rabbits; there was no adverse immunological response (*4*, *5*).

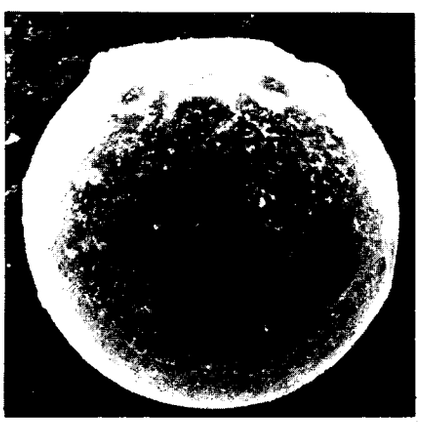

Fig. 1. A scanning electron micrograph of a norgestrel–serum albumin bead. The rough surface of the bead may be due to loosely adsorbed steroid or to abrasion of the polymer during stirring.

Progesterone (10 mg) was suspended in 0.8 ml of sodium phosphate buffer (1 m*M*, *p*H 7.5) containing sodium dodecyl sulfate (0.1 percent). Bovine serum albumin (200 mg) was then dissolved in the suspension and kept at 4°C. Polymerization was initiated by the addition of 0.2 ml of glutaraldehyde, making the final concentration 1 percent. The system was rapidly mixed, pipetted into 100 ml of an oil phase (corn oil and petroleum ether, 1:4 by volume), and stirred at room temperature. A water-in-oil emulsion formed. Although cross-linking of the protein in the emulsified droplets is complete in 10 minutes, the reaction mixture was stirred continuously for 1 hour before the oil phase was decanted. The resulting beads were washed three times with petroleum ether and dried in a vacuum desiccator. The size of the beads depends on the speed of stirring; the procedure outlined above consistently yielded beads with diameters of 100 to 200 μm (Fig. 1). Light microscopy at 100 times magnification revealed symmetrical beads with hormone crystals embedded in the matrix. The beads retained drug even after extensive washing with aqueous buffer solutions to get rid of excess reagents, as proved by release experiments in vitro. Drug content per milligram of beads can be controlled by varying the drug concentration in the reaction mixture. Beads with steroid concentrations of 5 to 30 percent were prepared in this manner.

For experiments in vivo, beads were prepared as described above, except that progesterone was entrapped in a matrix of serum albumin from rabbits. The steroid content was 20 percent of the bead weight. To facilitate the injection pro-

0036-8075/81/0710-0233$00.50/0